

*To appear in the Milan Journal of Mathematics*

# POLYHEDRA IN PHYSICS, CHEMISTRY AND GEOMETRY \*

Michael Atiyah <sup>†</sup> and Paul Sutcliffe <sup>‡</sup>

<sup>†</sup> *School of Mathematics,  
University of Edinburgh,  
King's Buildings, Edinburgh EH9 3JZ, U.K.  
Email : atiyah@maths.ed.ac.uk*

<sup>‡</sup> *Institute of Mathematics,  
University of Kent,  
Canterbury, CT2 7NZ, U.K.  
Email : P.M.Sutcliffe@kent.ac.uk*

February 2003

## Abstract

In this article we review some problems in physics, chemistry and mathematics that lead naturally to a class of polyhedra which include the Platonic solids. Examples include the study of electrons on a sphere, cages of carbon atoms, central configurations of gravitating point particles, rare gas microclusters, soliton models of nuclei, magnetic monopole scattering and geometrical problems concerning point particles.

---

\*Based on the Leonardo da Vinci Lecture given by the first author in Milan in October 2001.

# 1 Introduction

Polyhedra, particularly the Platonic solids, have been studied by geometers for thousands of years. Furthermore, finding physical applications of polyhedra is a similarly ancient pursuit. Plato was so captivated by the perfect forms of the five regular solids that in his dialogue *Timaeus* he associates them with what, at that time, were believed to be the basic elements of the world, namely, earth, fire, air, water and ether. Kepler also attributed cosmic significance to the Platonic solids. In his book *Mysterium Cosmographicum* he presents a version of the solar system as nested Platonic solids, the radii of the intervening concentric spheres being related to the orbits of the planets. This model had the compelling feature that the existence of only five Platonic solids explained why there were only the six planets known at that time. The models of both Plato and Kepler are, of course, entirely false, but more promising applications have since come to light.

Recently, there has been an increasing interest in a class of polyhedra, which include the Platonic solids, because they arise naturally in a number of diverse problems in physics, chemistry, biology and a variety of other disciplines. In this article we shall describe this class of polyhedra and some problems in physics, chemistry and mathematics which lead naturally to their appearance. As we do not discuss any applications to biology the interested reader may wish to consult the book by Weyl [43], for a general discussion of symmetry in the natural world. For a more technical example, a particularly interesting application of polyhedra in biology is provided by the structure of spherical virus shells, such as HIV which is built around a trivalent polyhedron with icosahedral symmetry [33, 20].

We begin, in the next Section, by recalling some details of the Platonic solids, before going on to discuss more general polyhedra. In the following Sections we then describe some applications in which these polyhedra arise. First, we deal with systems described by point particles. The particles have forces that act between them and we are interested in equilibrium states (usually stable ones) in which the particles sit at the vertices of certain polyhedra. To begin with we deal with 2-particle forces, such as the inverse square law, which describes both gravitational attraction and the repulsion of identical electric charges. To obtain polyhedral solutions with a single 2-particle force requires either a constraint on the particles, or an additional force, in order to balance the tendency to collapse or expand under the action of a single force. We describe examples of both situations and then turn to some geometric multi-particle forces which solve the scaling problem in a novel way, by being scale invariant. Finally, in Section 8, we move on from point particles and turn to classical field theories, discussing Skyrmin solutions and how they relate to polyhedra.

## 2 Platonic Solids and Related Polyhedra

A Platonic, or regular, solid is a polyhedron whose faces are identical regular polygons with all vertex angles being equal. There are precisely 5 Platonic solids, the tetrahedron, octahedron, cube, icosahedron and dodecahedron. In Table 1 we list the number of vertices,

Polyhedron	$V$	$F$	$E$
tetrahedron	4	4	6
octahedron	6	8	12
cube	8	6	12
icosahedron	12	20	30
dodecahedron	20	12	30

Table 1: The number of vertices  $V$ , faces  $F$  and edges  $E$  of the 5 Platonic solids.

faces and edges of the Platonic solids. Although they are termed Platonic solids there is convincing evidence that they were known to the Neolithic people of Scotland at least a thousand years before Plato, as demonstrated by the stone models pictured in fig. 1 which date from this period and are kept in the Ashmolean Museum in Oxford.

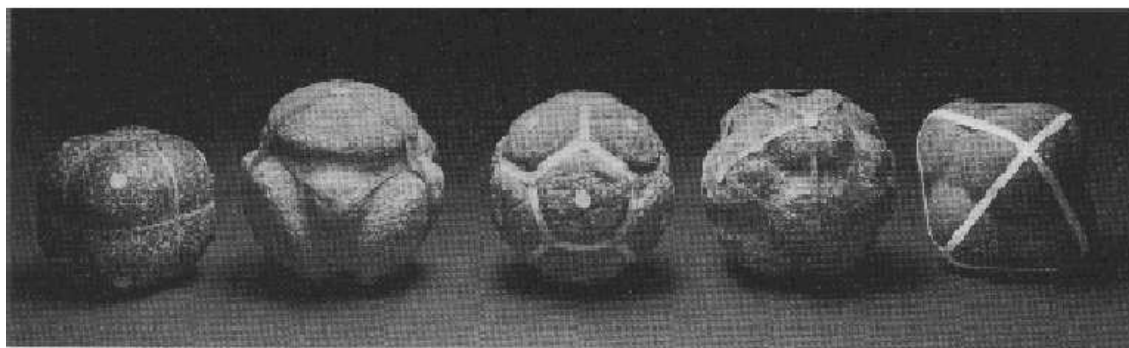


Figure 1: Stone models of the cube, tetrahedron, dodecahedron, icosahedron and octahedron. They date from about 2000BC and are kept in the Ashmolean Museum in Oxford.

The tetrahedron, octahedron and icosahedron all have triangular faces and are therefore examples of deltahedra. A deltahedron is a polyhedron with only triangular faces, and is called regular if all the triangles are equilateral. There are only 8 convex regular deltahedra, and the number of their vertices covers the range from 4 to 12, excluding 11. It is perhaps of interest to note that in 1813 Cauchy proved that any convex polyhedron is rigid, but it is known that there are non-convex polyhedra which are not rigid [12]. The cube has square faces and the faces of a dodecahedron are regular pentagons. The tetrahedron, cube and dodecahedron are trivalent polyhedra, which means that precisely 3 edges meet at every vertex.

For any polyhedron the number of vertices  $V$ , faces  $F$  and edges  $E$ , must satisfy Euler's formula, which states that

$$V + F - E = 2. \quad (2.1)$$

Given a polyhedron one can construct its dual, which is a polyhedron in which the locations of the vertices and face-centers are exchanged. The octahedron and cube are

dual to each other, as are the icosahedron and dodecahedron. The dual of a tetrahedron is again a tetrahedron. From the definitions given above it is clear that the dual of a deltahedron is a trivalent polyhedron.

The rotational symmetry groups of the tetrahedron, octahedron and icosahedron are finite groups of order 12, 24 and 60, which we denote by  $T$ ,  $O$  and  $Y$  respectively. Since the cube is dual to the octahedron then its symmetry group is also  $O$ , and, again by duality,  $Y$  is the symmetry group of the dodecahedron. Although there are only 5 Platonic solids there are an infinite number of polyhedra which are symmetric under the Platonic symmetry groups  $T$ ,  $O$ ,  $Y$ .

### 3 Particles on a Sphere

In this Section we consider a set of point particles whose positions are constrained in some way; the most natural physical constraint being that the particles are restricted to the surface of a unit sphere.

The first problem we discuss is a model for electrons on a sphere. This is often known as the Thomson problem, even though the problem which J.J. Thomson explicitly posed [40] is a little different to this one, and is described in the next Section. The origin of Thomson's name being attached to the study of electrons on a sphere appears to be the paper by Whyte [44], in which the term Thomson problem is used in this context.

Consider  $n$  particles, with positions  $\mathbf{x}_i$ ,  $i = 1, \dots, n$ , and constrained to lie on the surface of the unit sphere, so that  $|\mathbf{x}_i| = 1$  for all  $i$ . The particles have unit electric charge and therefore the total Coulombic energy (in suitable units) is given by

$$E_1 = \sum_i^n \sum_{j < i} \frac{1}{|\mathbf{x}_i - \mathbf{x}_j|}. \quad (3.1)$$

The Thomson problem is, for a given  $n$ , to find the positions  $\mathbf{x}_i$  so that this energy is minimal. The resulting points are then in equilibrium under the action of their mutual Coulomb repulsions, the only net forces acting on each particle being normal to the sphere upon which they are constrained to lie.

Obviously, if there are only two particles then they will sit at any pair of antipodal points on the sphere. For  $n = 3$  one finds that they sit at the vertices of an equilateral triangle on a great circle. For  $n = 4, 6, 12$  the points sit at the vertices of the Platonic solids, namely the tetrahedron, octahedron and icosahedron, respectively. For all  $n \geq 4$  the points sit at the vertices of a polyhedron, which is generically a deltahedron.

In fig.2 we display the associated polyhedra for  $n \leq 32$ . Note that  $n = 8$  is the first example in which the polyhedron is not a deltahedron, it being a square anti-prism, obtained from a cube by rotating the top face by  $45^\circ$  relative to the bottom face. This example demonstrates a general feature that the most symmetric configurations are not automatically those of lowest energy, since the more symmetric cube is not favoured for 8 points. Similarly, the dodecahedron is not obtained for 20 points, since it is far from possessing the deltahedral property which is clearly favoured.

$n$	$G$
2	$D_{\infty h}$
3	$D_{3h}$
4	$T_d$
5	$D_{3h}$
6	$O_h$
7	$D_{5h}$
8	$D_{4d}$
9	$D_{3h}$
10	$D_{4d}$
11	$C_{2v}$
12	$Y_h$
13	$C_{2v}$
14	$D_{6d}$
15	$D_3$
16	$T$
17	$D_{5h}$
18	$D_{4d}$
19	$C_{2v}$
20	$D_{3h}$
21	$C_{2v}$
22	$T_d$
23	$D_3$
24	$O$
25	$C_{1h}$
26	$C_2$
27	$D_{5h}$
28	$T$
29	$D_3$
30	$D_2$
31	$C_{3v}$
32	$Y_h$

Table 2: The symmetry group  $G$  of the configuration of  $n$  points which minimizes the energy of the Thomson problem, for  $2 \leq n \leq 32$ .

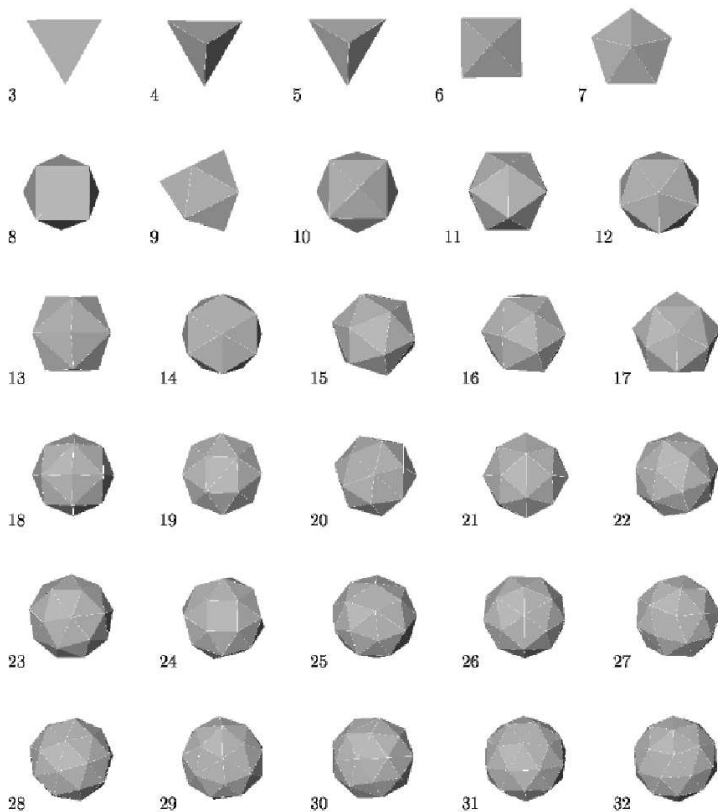


Figure 2: Polyhedra with vertices located at the  $n$  points on the sphere which minimize the energy of the Thomson problem for  $3 \leq n \leq 32$ .

In Table 2 we present the symmetries of the minimal energy configurations for  $n \leq 32$ , obtained from numerical simulations. To obtain the global minimum for large values of  $n$  is a notoriously difficult numerical problem, due to the fact that there is a rapid growth of local minima with increasing  $n$ . However, the use of modern computers has provided numerical results for  $n \leq 200$ , and their symmetries have been identified [36, 17]. The numerical methods used on this problem are numerous and varied, including multi-start conjugate gradient algorithms, simulated annealing and genetic codes. In fact, because of its complexity and richness, the Thomson problem is often used as a test problem in evaluating the efficiency of new numerical minimization algorithms.

In case the reader is not familiar with the notation used in Table 2 for the symmetry groups we briefly recount the main details here. The dihedral group  $D_k$  is obtained from the cyclic group of order  $k$ ,  $C_k$ , by the addition of a  $C_2$  axis which is orthogonal to the main  $C_k$  symmetry axis. The group  $D_k$  can be extended by the addition of a reflection symmetry in two ways: by including a reflection in the plane perpendicular to the main  $C_k$  axis, which produces the group  $D_{kh}$  or, alternatively, a reflection symmetry may be

imposed in a plane which contains the main symmetry axis and bisects the  $C_2$  axes, which results in the group  $D_{kd}$ . In the same way as for the dihedral groups the Platonic groups  $T, O, Y$ , which we introduced earlier, may also be enhanced by reflection symmetries, again denoted by the subscripts  $h, d$ . The addition of a subscript  $h$  to a cyclic group denotes a horizontal reflection symmetry, but a vertical reflection plane is denoted by a subscript  $v$ .

An obvious extension of the Thomson problem is to replace the Coulomb interaction (3.1) by a more general power law

$$E_p = \sum_i^n \sum_{j < i} \frac{1}{|\mathbf{x}_i - \mathbf{x}_j|^p}. \quad (3.2)$$

Again polyhedral solutions are obtained, but the symmetry and structure of the minimal energy configuration generally has an interesting non-trivial behaviour as a function of  $p$  (and  $n$ ) [32].

In the limit as  $p \rightarrow \infty$  the generalized problem (3.2) is equivalent to the Tammes problem, named after the Dutch botanist who posed the problem in connection with the study of pores in spherical pollen grains [39]. The Tammes problem is to determine the configuration of  $n$  points on a sphere so that the minimum distance between the points is maximized. This is equivalent to asking how to pack  $n$  identical circular caps on the surface of a sphere so that the diameter of the caps is as large as possible. As expected, polyhedral solutions are also obtained for the Tammes problem, but, perhaps surprisingly, for  $n > 6$  the numerical results suggest that the only configuration which is a common solution of the Coulomb and Tammes problem is the icosahedral arrangement for  $n = 12$  [17].

The final example that we mention for points on a sphere is a problem in discrete geometry which was first posed about fifty years ago by Fejes Tóth [19]. This problem is to maximize the sum of the mutual separations, or equivalently to minimize the energy

$$E_{-1} = - \sum_i^n \sum_{j < i} |\mathbf{x}_i - \mathbf{x}_j|. \quad (3.3)$$

The solutions of this problem are also polyhedral and usually, though not always, have the same symmetry group and combinatorial type as the solutions of the Thomson problem [36]. For example, the symmetry groups listed in Table 2, for  $2 \leq n \leq 32$ , are also the symmetry groups of this problem, excepts for the cases  $n = 7$  and  $n = 29$ . For the Thomson problem the  $n = 7$  polyhedron is a regular pentagonal bipyramid (see fig. 2) but for this problem the polyhedron is a symmetry breaking perturbation of this bipyramid, having only a  $C_2$  symmetry with 2 antipodal points and the remaining 5 points sprinkled around an equatorial band. The symmetry of the extremal configuration of 29 points is  $C_{2v}$  rather than the  $D_3$  symmetry of the Thomson problem.

There are a number of theorems proved about the extrema of the energy (3.3) and in particular there is the lower bound [1] for the minimum

$$E > \frac{1}{2} - \frac{2}{3}n^2, \quad (3.4)$$

which is also a reasonable estimate of the true minimal energy.

## 4 Central Configurations and Related Problems

In this Section we consider point particles whose positions are unconstrained, but which have an additional central force in order to balance a 2-particle interaction.

First, we consider central configurations, which are minima of the energy

$$E = \sum_i \sum_{j < i} \frac{1}{|\mathbf{x}_i - \mathbf{x}_j|} + \sum_i \frac{1}{2} \mathbf{x}_i^2, \quad (4.1)$$

where each point  $\mathbf{x}_i$ , for  $i = 1, \dots, n$ , is now unconstrained and so may take any value in  $\mathbb{R}^3$ . The variation of this energy yields the equilibrium equations

$$\mathbf{x}_i + \sum_{j \neq i} \frac{\mathbf{x}_j - \mathbf{x}_i}{|\mathbf{x}_i - \mathbf{x}_j|^3} = 0, \quad (4.2)$$

in which there is a balance between a repulsive inverse square force between the particles and a linear attraction to the origin.

One physical interpretation of the energy (4.1) arises when the inverse square force is thought of as an electrostatic repulsion between like charges and the linear force as an attraction due to a uniform background of the opposite charge. In this guise the problem originally arose in J.J. Thomson's static Plum Pudding model of the atom [40] in which the positive electric charge is smeared out into a uniform ball (the pudding) while the negatively charged electrons correspond to the plums. Although Rutherford's experiments conclusively demonstrated that this model is not relevant as a theory of atomic structure, it nevertheless continues to offer insights into the structure of metals (with the role of positive and negative charges interchanged) and other condensed matter systems and is often referred to as the One Component Plasma (OCP) model [8], or sometimes as classical Jellium.

An alternative interpretation of the equilibrium equations (4.2) is that it describes a force balance between gravitating point particles, with an attractive inverse square force law, and a repulsive radial force proportional to the distance from the origin. The repulsive linear force is such as arises in theories with a cosmological constant and also arises naturally if a time dependent homothetic ansatz is used in Newton's equations of motion. For the gravitational interpretation the appropriate potential function is  $-E$ , so minimizing  $E$  does provide critical configurations, that is, they are solutions of the equilibrium equations (4.2), but they are not minima of the gravitational energy  $-E$ . However, the issue of dynamical stability is more complicated in the gravitational setting. The actual particles are not static, because of the time dependent homothetic ansatz, so the instability of these solutions requires more than just the existence of a negative mode for the energy  $-E$ , and is by no means obvious.

It turns out that the electrostatic interpretation provides a useful insight into the properties of the configurations which minimize the energy (4.1). For example, a lower bound on the energy can be obtained by considering the packing of  $n$  non-overlapping Thomson



type Hydrogen atoms, that is, spheres with a single point charge at their centre but with zero total charge inside the sphere. This bound is given by [28, 5]

$$E \geq \frac{9}{10}n(n^{2/3} - 1) \quad (4.3)$$

and is a reasonably good estimate of the true minimal energy, indicating that the sphere packing assumption under which it is derived is a good description of the true minimizing configuration. For  $3 \leq n \leq 12$  the minimal energy configurations are displayed in fig. 3

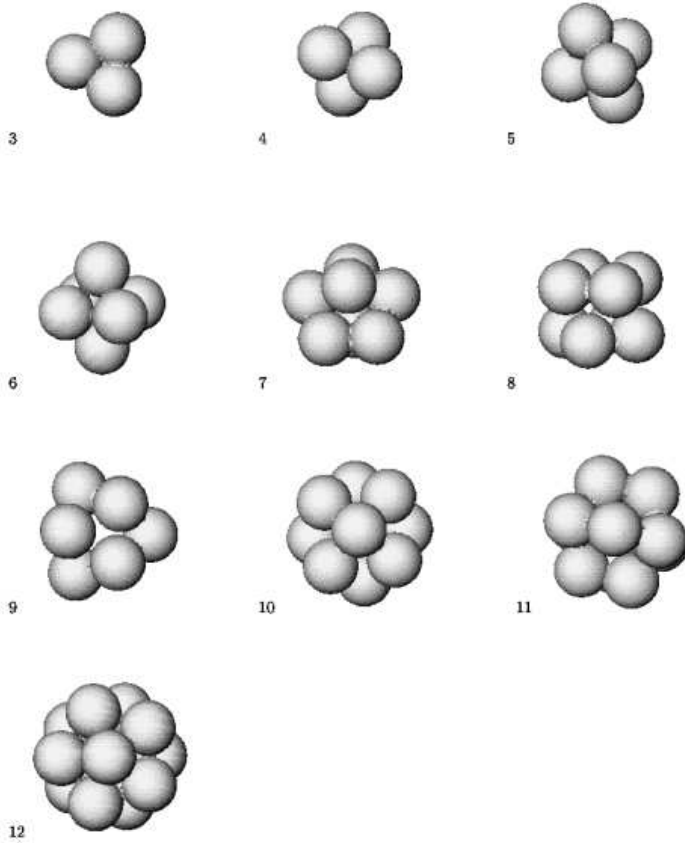


Figure 3: For  $3 \leq n \leq 12$  the minimal energy central configurations of  $n$  points are displayed by plotting spheres of diameter  $d = 1.65$  around each of the points.

by plotting spheres of diameter  $d = 1.65$  around each of the points. This illustrates the sphere packing nature of the solutions. The numerical value of 1.65 for the diameter  $d$  was determined using statistical data from configurations with large values of  $n$ , though analytic considerations lead to a similar value [5]. For  $n \leq 12$  all the points lie on, or very close to, the surface of a sphere and the symmetry and combinatoric type of each of the

configurations matches that for the Thomson problem. Thus for  $n < 13$  the polyhedra associated with this problem are essentially those of the Thomson problem. However, for  $n \geq 13$  this is no longer true and not all the points lie close to the surface of a single sphere. For example, at  $n = 13$  there are 12 points on the vertices of an icosahedron and an additional point at the origin. This may be thought of as a 2-shell structure, with the first shell containing a single point and the second shell containing 12 points. A 2-shell structure persists for all  $13 \leq n \leq 57$  and  $n = 60$ , with the arrangement of points within each shell resembling that for the Thomson problem. For example, for  $n = 32$  the inner shell contains 4 points on the vertices of a tetrahedron and the 28 points in the outer shell are also arranged in a tetrahedrally symmetric configuration, as suggested by the symmetry of the Thomson problem in Table 2. These two tetrahedral arrangements are appropriately aligned so that the whole structure has tetrahedral symmetry, and this gives the  $n = 32$  configuration a particularly low energy.

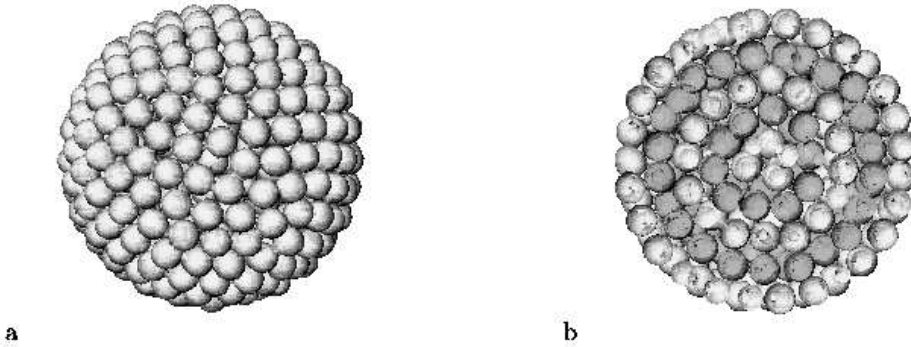


Figure 4: (a) A sphere packing presentation of a central configuration with 500 points. (b) A slice through the centre of this configuration, highlighting the 5 shells by alternately shading the shells light and dark grey.

The number of shells increases with  $n$  and so for  $n$  up to around 1000 points we may picture the configuration as points which sit at the vertices of a set of nested polyhedra. In fig. 4a we display, using the same sphere packing presentation as in fig. 3, a low energy local minimum configuration containing 500 points, which is a good candidate for the global minimum. In fig. 4b we present a slice through the centre of this configuration, highlighting the 5 shells by alternately shading the shells light and dark grey. At around 1000 points the shell-like structure begins to break down, with the distinction between the shells becoming blurred. For larger values of  $n$  the configuration resembles a random close packing of hard spheres, similar to Bernal's model of liquids. The configuration tends towards having a constant density, with 2-point and 3-point probability distributions agreeing to a high precision with those of a uniform distribution of points inside a ball [5]. There is numerical evidence [41] for a transition, at some value between 11000 and 15000 points, to a body

centred cubic structure as the minimal energy arrangement.

As we have seen, the points which minimize the energy (4.1) lie on the vertices of a single polyhedron only for  $n \leq 12$ , and for larger  $n$  nested polyhedra appear since the points do not all lie close to the surface of a single sphere. However, there is a variation of the central configuration energy which, for all values of  $n$ , does appear to have all the points lying close to the surface of a sphere [4]. This involves replacing the Coulomb energy, the first term in (4.1), by the energy (3.3), discussed in Section 3 when studying points on the sphere which maximize the sum of their mutual separations. The modified energy is given by

$$E = - \sum_i^n \sum_{j < i} |\mathbf{x}_i - \mathbf{x}_j| + \sum_i^n \frac{1}{2} \mathbf{x}_i^2, \quad (4.4)$$

where each of the  $n$  points  $\mathbf{x}_i$  is again unconstrained.

For the minimal energy configurations all  $n$  points lie on, or very close to, the surface of a sphere whose radius grows linearly with  $n$  and is well approximated by the formula  $r = \frac{2n}{3} - \frac{1}{2n}$ . The arrangement of the points is essentially the same as for the energy (3.3), when the points are constrained to lie precisely on this sphere. This observation allows the use of the estimate (3.4) to provide the approximation [4]

$$E = -\frac{2}{9}n^3 + \frac{1}{3}n - \frac{1}{8} \quad (4.5)$$

which is a good estimate of the true minimal energy value.

The energy function (4.4) appeared in the study of monopole scattering [4], as we now briefly describe. BPS monopoles are topological solitons in three space dimensions and the equation describing a static  $n$ -monopole solution has a moduli space of dimension  $4n$ . The  $4n$  parameters may be thought of as describing a position and phase for each of the  $n$  monopoles and the low energy scattering of monopoles can be approximated by geodesic motion on the moduli space [30]. For  $n$  fundamental monopoles in an  $SU(n+1)$  gauge theory the metric on the moduli space is the hyperkähler Lee-Weinberg-Yi metric [27], which is known explicitly. There are geodesics which describe a time dependent scaling solution, providing the monopole positions satisfy a set of algebraic constraints. These constraints are precisely the equations satisfied by the critical points of the energy function (4.4), and so minima of this energy yield geodesics, which have an interpretation in terms of monopole scattering, with the points identified as the positions of the monopoles. These solutions describe the scattering of  $n$  monopoles which lie on the vertices of a bouncing polyhedron; the polyhedron contracts from infinity to a point, representing the spherically symmetric  $n$ -monopole, and then expands back out to infinity.

## 5 Lennard-Jones Clusters

In the previous Section we studied unconstrained particles with a repulsive 2-body force and an additional linear force producing attraction to the origin. In this Section we discuss the situation in which the particles are acted upon by two 2-body forces with

opposite characters, that is, one force is repulsive and the other is attractive, leading to a finite non-zero separation at which two particles feel no mutual force.

A particularly interesting example is the Lennard-Jones interaction energy

$$E = \sum_i^n \sum_{j < i} \left\{ \frac{1}{|\mathbf{x}_i - \mathbf{x}_j|^{12}} - \frac{2}{|\mathbf{x}_i - \mathbf{x}_j|^6} \right\} \quad (5.1)$$

which is a good model for rare gas microclusters [22]. A microcluster is an aggregate of a small number of atoms, where an appreciable number of the atoms reside at the surface of the structure. For microclusters of rare gases the most relevant force which binds the atoms is a weak van der Waals force, and this is well approximated by the classical Lennard-Jones energy.

In (5.1) we have scaled the length and energy units so that two atoms a unit distance apart feel no mutual force. For  $3 \leq n \leq 7$  the symmetry of the energy minimizing configuration agrees with that shown in Table 2, with the atoms sitting at the vertices of an equilateral triangle, tetrahedron, triangular bipyramid, octahedron and pentagonal bipyramid respectively, in qualitative agreement with the polyhedra displayed in fig. 2. However, for  $n \geq 8$  the structures which emerge are, generically, quite different from the problems we have considered so far, although they are connected to polyhedra in a slightly different way.

The minimal energy arrangement of atoms is, almost always, obtained from a filling and partial filling of the vertices of Mackay icosahedra. Consider a sphere surrounded by 12 identical spheres on the vertices of an icosahedron. As pointed out by Mackay [29] one may consider the icosahedron as the first shell in a sequence of shells,  $s = 1, 2, 3, \dots$ . Each shell contains  $10s^2 + 2$  spheres and is packed around the previous one in a way that preserves the icosahedral symmetry. Clearly this leads to a sequence of numbers 13, 55, 147, ... in which an outer shell and all inner shells are completely filled. These complete Mackay icosahedra are the minimal energy Lennard-Jones configurations for these special values of  $n$ . In fig. 5 we present the  $n = 55$  Lennard-Jones cluster by plotting spheres of unit diameter around each of the 55 atoms. The outer shell containing 42 atoms is visible and surrounds 12 atoms on the vertices of an icosahedron with a single atom at its centre. Remarkably, as first demonstrated by Northby [34], partially filling the outer shell and completely filling the inner shells often produces the minimal energy configuration. For example, the minimal energy arrangement for 12 atoms is obtained from the  $n = 13$  Mackay icosahedron by removing an atom from a vertex of the icosahedron, not by removing the atom at the centre. Thus the symmetry of the  $n = 12$  minimal energy configuration is only  $C_{5v}$  and not the more symmetric icosahedral arrangement obtained by placing all 12 atoms on the vertices of an icosahedron.

There are a few values of  $n$  for which the minimal energy configuration is not based on Mackay icosahedra [15] and these are difficult to find numerically because of the enormous number of local minima which exist for this problem. For example, even at  $n = 13$  numerical methods have computed 1467 different local minima [14].

Using electron diffraction techniques experimental studies [18] of argon microclusters in nozzle beams have revealed a remarkable agreement with the icosahedral based structures

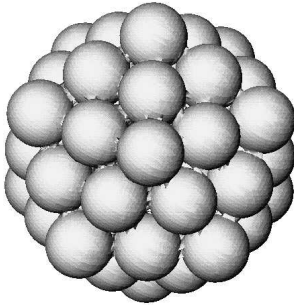


Figure 5: The Lennard-Jones cluster for 55 atoms. Each atom is represented by a sphere of unit diameter.

predicted by minimization of the simple Lennard-Jones energy. Also, intensity anomalies coincide with the particularly stable atom numbers associated with complete Mackay icosahedra.

## 6 Geometric Energies

So far we have seen two situations in which minimal energy configurations have the particles located at the vertices of a single polyhedron. The first is where the particles are constrained to lie on the surface of a sphere and the second is the energy (4.4) in which a 2-body repulsive force for unconstrained particles is balanced by an attraction towards the origin. In this Section we describe some geometric energies with multi-particle forces which produce polyhedral minimizers and solve the scaling problem in a novel way, by being scale invariant.

To construct our first geometric energy consider  $n$  distinct ordered points,  $\mathbf{x}_i \in \mathbb{R}^3$  for  $i = 1, \dots, n$ . For each pair  $i \neq j$  define the unit vector

$$\mathbf{v}_{ij} = \frac{\mathbf{x}_j - \mathbf{x}_i}{|\mathbf{x}_j - \mathbf{x}_i|} \quad (6.1)$$

giving the direction of the line joining  $\mathbf{x}_i$  to  $\mathbf{x}_j$ . Now let  $t_{ij} \in \mathbb{CP}^1$  be the point on the Riemann sphere associated with the unit vector  $\mathbf{v}_{ij}$ , via the identification  $\mathbb{CP}^1 \cong S^2$ , realized as stereographic projection. Next, set  $p_i$  to be the polynomial in  $t$  with roots  $t_{ij}$  ( $j \neq i$ ), that is

$$p_i = \alpha_i \prod_{j \neq i} (t - t_{ij}) \quad (6.2)$$

where  $\alpha_i$  is a certain normalization coefficient (see ref.[3] for full details). In this way we have constructed  $n$  polynomials which all have degree  $n - 1$ , and so we may write  $p_i = \sum_{j=1}^n d_{ij} t^{j-1}$ . Finally, let  $d$  be the  $n \times n$  matrix with entries  $d_{ij}$ , and let  $D$  be its determinant

$$D(\mathbf{x}_1, \dots, \mathbf{x}_n) = \det d. \quad (6.3)$$

This geometrical construction is relevant to the Berry-Robbins problem [9], which is concerned with specifying how a spin basis varies as  $n$  point particles move in space, and supplies a solution provided it can be shown that  $D$  is always non-zero. For  $n = 2, 3, 4$  it can be proved that  $D \neq 0$  [2, 16] and numerical computations [3] suggest that  $|D| \geq 1$  for all  $n$ , with the minimal value  $|D| = 1$  being attained by  $n$  collinear points.

The geometric energy is the  $n$ -point energy defined by

$$E = -\log |D|, \quad (6.4)$$

so minimal energy configurations maximize the modulus of the determinant.

This energy is geometrical in the sense that it only depends on the directions of the lines joining the points, so it is translation, rotation and scale invariant. Remarkably, the minimal energy configurations, studied numerically [3] for all  $n \leq 32$ , are essentially the same as those for the Thomson problem displayed in fig. 2. The points lie on, or very close to, the surface of a sphere, though of course the radius and centre of the sphere are now arbitrary. The symmetries and combinatorial types agree in all cases and plots of the associated polyhedra cannot be distinguished from those in fig. 2. It is expected that the points lie close to the surface of a sphere for all values of  $n$ , though the numerical evidence is currently only available for  $n \leq 32$ . It would be interesting to see if the similarity with the Thomson problem continues for larger values of  $n$ , or whether some qualitative differences arise for  $n$  sufficiently large.

A fairly accurate approximation to the minimal energy value is obtained using the quadratic fit

$$E(n) = -an^2 + bn + 4a - 2b \quad (6.5)$$

where  $a = 0.143$  and  $b = 0.792$ .

The geometrical energy (6.4) may be interpreted as a volume in a higher dimensional space [3] and this point of view may provide a new perspective on configurations in the Thomson problem.

Often a complicated multi-particle energy function can be expanded as a sum of pure  $k$ -particle energies, starting with  $k = 2$ , which may be the dominant contribution. For just 2 particles the geometrical energy (6.4) is independent of their positions, so an expansion in terms of  $k$ -particle energies must start with  $k = 3$ . For 3 points the energy (6.4) may be written as [2]

$$E^{(3)} = -\log\left\{\frac{3}{4} + \frac{1}{4}(\cos\theta_1 + \cos\theta_2 + \cos\theta_3)\right\} \quad (6.6)$$

where  $\theta_1, \theta_2, \theta_3$  are the angles in the triangle formed by the 3 points. In this form it is clear that the minimal value of  $E^{(3)}$  is  $-\log(9/8)$ , obtained by the equilateral triangle  $\theta_1 = \theta_2 = \theta_3 = \pi/3$ . The fact that this 3-particle energy might be the dominant part of the full energy (6.4) motivates the study of the second geometrical energy

$$E_\Delta = \frac{-6}{n(n-1)(n-2)} \sum_{i>j>k} \log\left\{\frac{3}{4} + \frac{1}{4}(\cos\theta_i + \cos\theta_j + \cos\theta_k)\right\} \quad (6.7)$$

where  $\theta_1, \theta_2, \theta_3$  are the angles in the triangle formed by the 3 points  $\mathbf{x}_i, \mathbf{x}_j, \mathbf{x}_k$ . The sum runs over all triples of points and the prefactor counts the number of triples, so that the energy is the average 3-particle energy per triangle. A numerical study [3] of the minimal energy configurations for the triangular energy (6.7) confirms that it reproduces the arrangements of points for the full energy (6.4) to a good accuracy, with the positions of all the particles differing by less than 1% in all cases.

It is intriguing that the 3-particle energy (6.6) has arisen in a different physical context [11]. This concerns quantum many-body problems for which eigenstates can be found explicitly. It turns out that the addition of precisely this 3-body interaction allows the explicit computation of some eigenstates (including the ground state) of less tractable Hamiltonians with only 2-body forces.

Minimal energy configurations for the multi-particle energy (6.4) may also be studied for  $n$  points in the plane. The results for  $2 \leq n \leq 15$  are perhaps not surprising, with the  $n$  points lying on a circle and forming the vertices of a regular  $n$ -gon. However, for  $n = 16$  the minimal energy configuration consists of a regular 15-gon on a circle and a single point at the origin. The pattern of an  $(n - 1)$ -gon plus one point at the centre continues until  $n = 23$ , at which point the configuration comprises a 21-gon plus 2 points placed in the interior of the circle equidistant from its centre and lying on a diameter. At  $n = 28$  a further point enters the interior of the circle, producing a 25-gon with an equilateral triangle inside. At  $n = 33$  another point enters the interior of the circle, leading to a 29-gon with a square arrangement at the interior. Note that the points in the interior are always arranged in the minimal energy configuration of that number. We refer to the sequence of numbers,  $n = 16, 23, 28, 33, \dots$  at which an additional point enters the interior of the circle, as the jumping values.

These planar configurations are qualitatively similar to the global minima for the Coulomb energy (3.1) for point charges in a disk [35]. The same patterns of points emerge in the Coulomb case, though the jumping values are shifted to the sequence  $n = 12, 17, 19, 22, \dots$ . Thus the jumps occur earlier and more frequently for the Coulomb energy. In the Coulomb problem the number of shells increases for even larger values of  $n$  and we expect a similar phenomenon for the planar geometric energy.

## 7 Fullerenes

A particularly interesting class of trivalent polyhedra occur with  $F$  faces where  $F \geq 12$ . They are composed of 12 pentagons and  $F - 12$  hexagons. The trivalent property together with Euler's formula (2.1) then determines that the numbers of vertices and edges are given by  $V = 2F - 4$  and  $E = 3F - 6$ . We refer to a polyhedron of this type as a Fullerene polyhedron, the name being taken from a particular application which we shall discuss in this Section. The first Fullerene polyhedron has  $F = 12$  and is the dodecahedron. Another interesting Fullerene with icosahedral symmetry occurs when  $F = 32$ , and is the truncated icosahedron, which can be obtained from an icosahedron by 'chopping off' each of the 12 vertices, leaving 12 pentagons and 20 hexagons. The number of combinatorially different

Fullerenes grows rapidly with  $F$ . For example, although the dodecahedron is the unique Fullerene with  $F = 12$ , there are already 40 different Fullerenes with  $F = 22$  [21]. Clearly, the dual of a Fullerene is a deltahedron in which either 5 or 6 triangles surround a vertex, these two cases being termed pentamers and hexamers respectively. The polyhedra which have arisen in previous Sections, with vertices given by the positions of energy minimizing point particles, are therefore generically dual to Fullerene polyhedra, once the number of particles is at least 20.

Fullerene polyhedra have become of great interest in recent years due to their unexpected appearance in carbon chemistry. Natural carbon can exist in several forms, such as graphite and diamond, but there is another form, called Fullerenes. Fullerenes are large carbon-cage molecules, by far the most common being the  $C_{60}$  buckyball [26], whose discovery was rewarded with the 1996 Nobel Prize in Chemistry. The carbon atoms sit at the vertices of a Fullerene polyhedron (as defined above), with the bonds represented by the edges of the polyhedron. Although carbon is quadrivalent, the polyhedron is trivalent since each carbon atom is linked to two others by a single bond and to one further carbon atom by a double bond; the difference in lengths between a double and single bond is small and so can be neglected. As an example, the 60 atoms in the buckyball are located on the vertices of a truncated icosahedron, a model of which is displayed in fig. 6. Other Fullerenes

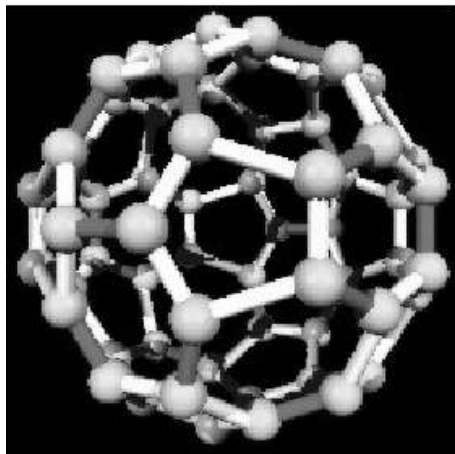


Figure 6: A model of the  $C_{60}$  buckyball.

are also common, particularly  $C_{70}$ ,  $C_{76}$  and  $C_{84}$ , and have been found to exist in interstellar dust as well as in geological formations on Earth. As mentioned above, there is a rapid growth in the number of different Fullerenes as the number of carbon atoms increases, and it is a challenging task to catalogue and understand the properties of all possible Fullerenes, as well as predict, by energy minimization, those most likely to be found in experiments. However, simple geometrical rules, such as separating the pentagonal faces, appear to play an important role [45].



## 8 Skyrmions

In the previous Sections we have dealt with energy minimizing configurations of point particles, but in this Section we turn to a classical field theory whose solutions are also related to polyhedra.

The Skyrme model [37] is a nonlinear field theory whose classical soliton solutions, called Skyrmions, are candidates for an effective description of nuclei with an identification between the number of nucleons and solitons.

The basic field of the model is a 4-component unit vector,  $\phi(\mathbf{x}) = (\phi_1, \phi_2, \phi_3, \phi_4)$  with  $\phi \cdot \phi = 1$ . The field is defined throughout  $\mathbb{R}^3$  and satisfies the boundary condition that  $\phi \rightarrow (0, 0, 0, 1)$  as  $|\mathbf{x}| \rightarrow \infty$ . This boundary condition compactifies space so that topologically  $\phi$  is a map between two 3-spheres. This map has an integer-valued winding number,  $B$ , which is just the degree of the map, and counts the number of solitons in a given field configuration. In the application to nuclear physics,  $B$  is identified with baryon number, that is, the number of nucleons.

The image under  $\phi$  of an infinitesimal sphere of radius  $\epsilon$  and centre  $\mathbf{x} \in \mathbb{R}^3$ , to leading order in  $\epsilon$ , is an ellipsoid with principal axes  $\epsilon\lambda_1, \epsilon\lambda_2, \epsilon\lambda_3$ .

In terms of this deformation the baryon number can be computed as the integral

$$B = \frac{1}{2\pi^2} \int \lambda_1 \lambda_2 \lambda_3 \, d^3x \quad (8.1)$$

and the static energy of the model is defined to be [31]

$$E = \frac{1}{12\pi^2} \int \lambda_1^2 + \lambda_2^2 + \lambda_3^2 + \lambda_1^2 \lambda_2^2 + \lambda_2^2 \lambda_3^2 + \lambda_3^2 \lambda_1^2 \, d^3x. \quad (8.2)$$

A simple inequality shows that the energy is bounded from below by the baryon number,

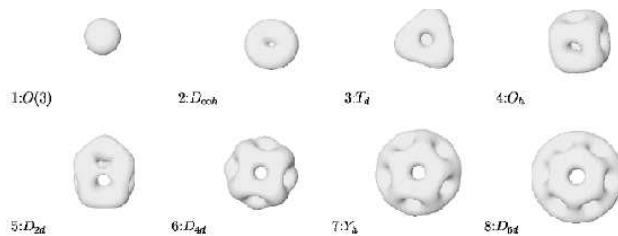


Figure 7: Baryon density isosurfaces for the minimal energy Skyrmions with  $1 \leq B \leq 8$ .

that is,  $E \geq B$ , which is known as the Faddeev-Bogomolny bound. It is easy to see that this bound can not be attained for any non-trivial field configuration. The mathematical problem is to compute, for a given integer  $B$ , the minimal energy field configuration with baryon number  $B$ . Using numerical methods, and a powerful parallel machine, minimal energy Skyrmions have been computed [7] for all  $B \leq 22$ . In fig. 7 we present surfaces of

constant baryon density (the integrand in equation (8.1)) for the minimal energy Skyrmions with  $1 \leq B \leq 8$ . Each Skyrmion is also labelled by the point symmetry group of the baryon density (or equivalently energy density).

The  $B = 1$  Skyrmion is spherically symmetric [37] but for  $B = 2$  the Skyrmion has only an axial symmetry [25, 42], with a toroidal structure for the baryon density isosurface. For  $B > 2$  the baryon density is localized around the edges (and especially vertices) of a polyhedron, which for  $B = 3$  and  $B = 4$  is a tetrahedron and cube respectively [10]. From fig. 7 it can be seen that each of the polyhedra is trivalent and contains  $2B - 2$  faces. This suggests a possible connection with Fullerene polyhedra which have  $F = 2B - 2$  faces, or equivalently  $V = 4B - 8$  vertices, for  $B \geq 7$ . In fig. 8 we present baryon density isosurfaces for minimal energy Skyrmions with  $7 \leq B \leq 22$ , together with models of the associated polyhedra. Generically, the polyhedra are of the Fullerene type, for example,  $B = 7$  is the dodecahedron and  $B = 17$  has  $V = 60$  vertices forming the truncated icosahedron of the buckyball. Two of the configurations are not of the Fullerene type ( $B = 9, 13$ ), as they contain quadrivalent vertices, but they can be understood as deformations of Fullerene polyhedra [7]. The baryon density isosurfaces displayed in fig. 7 are qualitatively similar to energy density isosurfaces for BPS magnetic monopoles [38], which are another kind of soliton. The equation for static monopoles is integrable and this allows exact results to be proved for monopoles, which can then be used as a guide for studying Skyrmions. In particular, there is an exact correspondence between the moduli space of static  $B$ -monopoles, and degree  $B$  rational maps between Riemann spheres [13, 24]. This motivated the development of an approximate ansatz for Skyrmions in terms of rational maps [23], which has proved remarkably successful in capturing both the qualitative and quantitative features of Skyrmions. Furthermore, this ansatz depends on only a (small) finite number of parameters, and induces an energy function on the moduli space of rational maps. Thus numerical computations of minimal energy maps can be performed with much less effort than minimizing the full Skyrme energy function, and yet produce results which are in good agreement with the full field theory [7].

A Skyrmion polyhedron has  $2B - 2$  faces, so taking its dual yields, generically, a deltahedron with  $n = 2B - 2$  vertices. An inspection of the symmetries of the minimal energy Skyrmions, presented in the labels in figs. 7 and 8, shows that quite often the symmetry of the minimal energy  $B$ -Skyrmion agrees with the symmetry of the solution of the Thomson problem (see Table 2) for  $n = 2B - 2$  particles on the sphere. More precisely, the symmetries match for the two problems in 17 out of the 22 cases. Moreover, a closer inspection reveals that in these 17 cases not only do the symmetry groups match, but the combinatorial types of the Skyrmion polyhedron and the dual of the Thomson polyhedron are identical. The 5 examples that do not coincide,  $B = 5, 9, 10, 19, 22$  shows that the topography of the two energy functions is slightly different and suggests that the same factors which determine the polyhedron (or its dual) are important, but perhaps with slightly different weightings. The fact that there is often an agreement for the two problems motivated the study [6] of icosahedral Skyrmions with values of  $B$  for which the solution of the Thomson problem with  $n = 2B - 2$  points has icosahedral symmetry. The results appear to support a connection between the two problems and suggests icosahedral

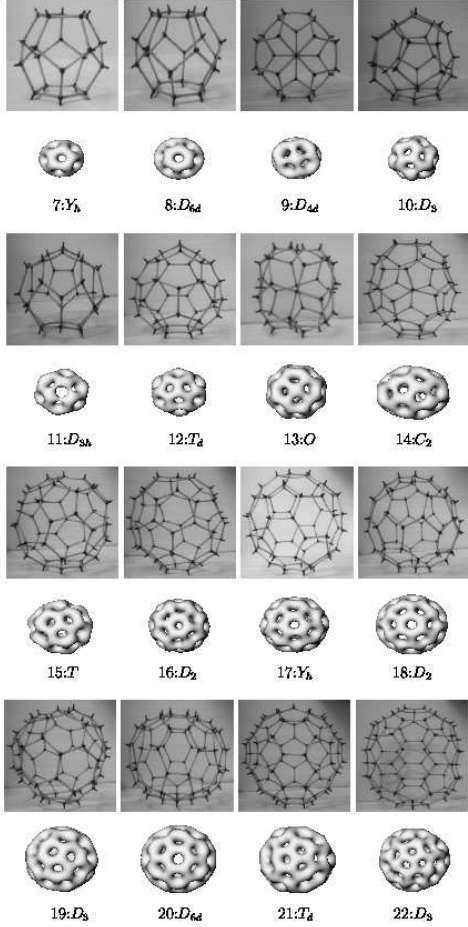


Figure 8: Baryon density isosurfaces for minimal energy Skyrmons with  $7 \leq B \leq 22$ , together with models of the associated polyhedra.

candidates for minimal energy Skyrmons with certain large values of  $B$ . As an example, the baryon density isosurface shown in fig. 9 is an icosahedrally symmetric Skyrmon with  $B = 97$ . It has very low energy and is a good candidate for the minimal energy 97-Skyrmion.

## 9 Conclusion

In this review we have discussed a range of problems in physics, chemistry and mathematics which all yield polyhedral solutions. Mainly, the problems we have addressed concern minimizing the energy of point particles, with the result that the particles are arranged on the vertices of a polyhedron. Sometimes the system involves a single repulsive

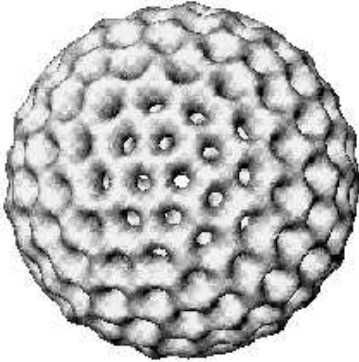


Figure 9: Baryon density isosurface for a  $B = 97$  Skyrmion with icosahedral symmetry.

2-particle interaction, and the points are constrained to lie on the surface of a sphere, so the emergence of a polyhedron is perhaps not so surprising – though the patterns and symmetries of the polyhedra often are. Perhaps more surprising, is the emergence of polyhedra when no constraints are placed on the particle positions, and yet the particles continue to be arranged on, or very close to, the surface of a sphere, and yield virtually the same polyhedral solutions. We also discussed a field theory in which polyhedra arise in a slightly different context, as structures around which the charge density of a soliton solution is localized, and mentioned an example of how a comparison with point particle systems can be used to gain some insight.

Even very simple interactions can yield complex structures and surprising results. Although the use of modern computers is vital in determining minimal energy arrangements, often a geometrical point of view can lead to new insights. As we have seen, on many occasions the geometry can be universal and progress made in one area can be directly applied to several different situations, leading to advances in a wide range of apparently unrelated disciplines.

## Acknowledgements

PMS acknowledges the EPSRC for an advanced fellowship.

## References

- [1] R. Alexander, *Acta Math. Acad. Sci. Hungar.* 23, 443 (1972).
- [2] M.F. Atiyah, *Phil. Trans. R. Soc. Lond. A* 359, 1 (2001).
- [3] M.F. Atiyah and P.M. Sutcliffe, *Proc. R. Soc. A* 458, 1089 (2002).

- [4] R.A. Battye, G.W. Gibbons, P. Rychenkova and P.M. Sutcliffe, hep-th/0212106, to appear in J. Math. Phys. (2003).
- [5] R.A. Battye, G.W. Gibbons and P.M. Sutcliffe, hep-th/0201101, to appear in Proc. Roy. Soc. A. (2003).
- [6] R.A. Battye, C.J. Houghton and P.M. Sutcliffe, hep-th/0210147, to appear in J. Math. Phys. (2003).
- [7] R.A. Battye and P.M. Sutcliffe, Phys. Rev. Lett. 86, 3989 (2001); Rev. Math. Phys. 14, 29 (2002).
- [8] M. Baus and J.-P. Hansen, Physics Reports 59, 1 (1980).
- [9] M.V. Berry and J.M. Robbins, Proc. R. Soc. A 453, 1771 (1997).
- [10] E. Braaten, S. Townsend and L. Carson, Phys. Lett. B 235, 147 (1990).
- [11] F. Calogero and C. Marchioro, J. Math. Phys. 14, 182 (1973).
- [12] R. Connelly, Math. Intelligencer 1, 130 (1978).
- [13] S.K. Donaldson, Commun. Math. Phys. 96, 387 (1984).
- [14] J.P.K. Doye, M.A. Miller and D.J. Wales, J. Chem. Phys. 111, 8417 (1999).
- [15] J.P.K. Doye, D.J. Wales and R.S. Berry, J. Chem. Phys. 103, 4234 (1995).
- [16] M. Eastwood and P. Norbury, Geom. Topol. 5, 885 (2001).
- [17] T. Erber and G.M. Hockney, Adv. Chem. Phys. 98, 495 (1997).
- [18] J. Farges, M.F.deFeraudy, B. Raoult and G. Torchet, J. Chem. Phys. 78, 5067 (1983).
- [19] L. Fejes Tóth, Acta Math. Acad. Sci. Hungar. 7, 397 (1956).
- [20] M.J. Forster, B. Mulloy and M.V. Nermut, J. Mol. Biol. 298, 841 (2000).
- [21] P.W. Fowler and D.E. Manolopoulos, *An Atlas of Fullerenes*, Clarendon Press (1995).
- [22] M.R. Hoare, Adv. Chem. Phys. 40, 49 (1979).
- [23] C.J. Houghton, N.S. Manton and P.M. Sutcliffe, Nucl. Phys. B 510, 507 (1998).
- [24] S. Jarvis, J. Reine Angew. Math. 524, 17 (2000).
- [25] V.B. Kopeliovich and B.E. Stern, JETP Lett. 45, 203 (1987).
- [26] H.W. Kroto, J.R. Heath, S.C. O'Brien, R.F. Curl and R.E. Smalley, Nature 318, 354 (1985).

- [27] K. Lee, E.J. Weinberg and P. Yi, Phys. Rev. D 54, 1633 (1996).
- [28] E.H. Lieb and H. Narnhofer, Journal of Statistical Physics 12 (1975) 291; Erratum in 14, 465 (1976).
- [29] A.L. Mackay, Acta Crystallogr. 15, 916 (1962).
- [30] N.S. Manton, Phys. Lett. B 110, 54 (1982).
- [31] N.S. Manton, Comm. Math. Phys. 111, 469 (1987).
- [32] T.W. Melnyk, O. Knop and W.R. Smith, Can. J. Chem. 55, 1745 (1977).
- [33] M.V. Nermut, D.J. Hockley, J.B.M. Jowett, I.M. Jones, M. Garreau and D. Thomas, Virology 198, 288 (1994).
- [34] J.A. Northby, J. Chem. Phys. 87, 6166 (1987).
- [35] K.J. Nurmela, J. Phys. A 31, 1035 (1998).
- [36] E.A. Rakhmanov, E.B. Saff and Y.M. Zhou, ‘*Electrons on the sphere*’, in ‘*Computational Methods and Function Theory*’, World Scientific (1995).
- [37] T.H.R. Skyrme, Proc. Roy. Soc. A 260, 127 (1961).
- [38] P.M. Sutcliffe, Int. J. Mod. Phys. A 12, 4663 (1997).
- [39] P.M.L. Tammes, Recueil Travaux Botaniques Neerlandais 27, 1 (1930).
- [40] J.J. Thomson, Philos. Mag. 7, 237 (1904); Philos. Mag. 41, 510 (1921).
- [41] H. Totsuji, T. Kishimoto, C. Totsuji and K. Tsuruta, Phys. Rev. Lett. 88, 125002 (2002).
- [42] J.J.M. Verbaarschot, Phys. Lett. B 195, 235 (1987)
- [43] H. Weyl, ‘*Symmetry*’, Princeton University Press (1952).
- [44] L.L. Whyte, Amer. Math. Monthly 59, 606 (1952).
- [45] B.L. Zhang, C.Z. Wang, K.M. Ho, C.H. Xu and C.T. Chan, J. Chem. Phys. 97, 5007 (1992).